CCFE
CULHAM CENTRE FOR FUSION ENERGY

UK Atomic Energy Authority

UKAEA-CCFE-PR(23)120

D. Brunetti, J. P. Graves, C. J. Ham, S. Saarelma

Occam's razor on the mechanism of Resistive Wall Mode induced limits in diverted tokamaks

Occam's razor on the mechanism of Resistive Wall Mode induced limits in diverted tokamaks

D. Brunetti, J. P. Graves, C. J. Ham, S. Saarelma

This is a preprint of a paper submitted for publication in
Physical Review Letters

Occam's razor on the mechanism of Resistive Wall Mode induced β limits in diverted tokamaks

D. Brunetti,[1,*] J. P. Graves,[2,3] C. J. Ham,[1] and S. Saarelma[1]

[1]UKAEA-CCFE, Culham Science Centre, Abingdon, Oxon, OX14 3DB, United Kingdom
[2]École Polytechnique Fédérale de Lausanne (EPFL),
Swiss Plasma Center (SPC), CH-1015 Lausanne, Switzerland
[3]York Plasma Institute, Department of Physics, University of York, York, Heslington, YO10 5DD, United Kingdom

(Dated: December 2, 2022)

External kink modes, believed to be the drive of the β-limiting Resistive Wall Mode, are strongly stabilised by the presence of a separatrix. We thus propose a novel mechanism explaining the appearance of long-wavelength global instabilities in free boundary high-β diverted tokamaks, retrieving the experimental observables within a physical framework dramatically simpler than most of the models employed for the description of such phenomena. It is shown that the magneto-hydrodynamic stability is worsened by the synergy of β and plasma resistivity, with wall effects significantly screened in an ideal, i.e. with vanishing resistivity, plasma with separatrix. Stability can be improved by toroidal flows, depending on the proximity to the resistive marginal boundary. The analysis is performed in tokamak toroidal geometry, and includes averaged curvature and essential separatrix effects.

Maximising β, the ratio of plasma pressure over kinetic pressure, is of crucial importance for an economically viable tokamak reactor, allowing a larger fraction of bootstrap current and higher fusion power yield. The maximum achievable β, however, is limited by the onset of global macroscopic magnetohydrodynamic (MHD) instabilities. Experimental evidence shows that this macroscopic pressure driven activity i) has an external component, ii) grows on time scales of the order of tens of milliseconds [1], iii) rotates slowly compared to the bulk plasma [2], iv) is stabilised by plasma rotation (even modest in some cases) [2, 3], and v) is triggered when β crosses a threshold which is smaller than the one predicted by ideal MHD stability analyses with a close fitting ideal wall [2].

The general consensus for this β limiting instability invokes a special form of the external kink (XK) mode enhanced by β effects as its most likely cause, with the magnetic flux diffusion through the resistive wall surrounding the plasma slowing down the fast growth of the XK [2]. This is known as the Resistive Wall Mode (RWM). Several theories have been proposed to explain such MHD phenomenon, see e.g. [2, 4–8]. Most of those have been developed in cylindrical geometry, and generally neglect plasma inertia and pressure effects [6] apart from few works which account for localised finite β corrections [5]. Only few analyses deal with proper toroidicity [7–10], although using peculiar equilibrium profiles and allowing mode resonances in the vacuum region.

For the RWM, viewed as a form of an XK, a fundamental role is played by the free energy contribution of the vacuum region. However, although external kinks are certainly possible in limited toroidal plasmas, extra care has to be taken when dealing with diverted geometries. With an x-point, the safety factor profile diverges at the separatrix. This constrains any mode of helicity $m/n > q_{min}$ (m and n are the toroidal and poloidal mode numbers and q_{min} is the minimum value of the safety factor) to resonate within the plasma. Therefore, in an ideal diverted plasma the XK is expected to be suppressed, and wall effects strongly reduced [11]. In numerical modelling a cut-off in the simulation domain is often introduced in order to avoid the edge singularity in q. The choice of this cut-off is usually such that q at the edge corresponds to the value of q at 95% of the normalised poloidal flux (q_{95}). Unfortunately, this introduces a degree of arbitrariness since results may depend strongly on the choice of q_{95} [12, 13].

Hence, in this Letter a new mechanism, featuring both internal and external characteristics, which explains the appearance of low-frequency long-wavelength macroscopic instabilities in a high-β diverted tokamak avoiding the arbitrariness of the choice of the edge q is presented. This framework retrieves all experimentally observed features associated with RWMs phenomena, although being significantly simpler than most of the models commonly employed for the interpretation of such dynamics. The analysis, performed in toroidal geometry within the *infernal model* framework [14, 15], naturally identifies pressure as the key driving player, with plasma resistivity both deteriorating stability and allowing the perturbation to have external-like features. Contrarily to the toroidal derivations of Refs. [7, 8], coupling occurs well inside the core region far from the innermost resonance and no modes are allowed to resonate in the vacuum. Our model accounts also for favourable averaged curvature effects, namely a negative Glasser-Greene-Johnson (GGJ) interchange parameter [16], and a sheared toroidal flow. Mode suppression can be achieved with modest rotation values if the resistive plasma is not too far from its marginal stability boundary.

We analyse a circular tokamak plasma of major and mi-

nor radii R_0 and a respectively in the limit of large aspect ratio ($\varepsilon = a/R_0 \ll 1$). The ordering $\beta = 2\mu_0 p/B_0^2 \sim \varepsilon^2$ is adopted, where p is the plasma pressure and B_0 the magnetic field strength on the axis. A right handed straight field line coordinate system (r, ϑ, ϕ) is introduced with r a flux label with the dimensions of length, and ϑ (counter-clockwise in the poloidal cross-section) and ϕ the poloidal-like and toroidal angles respectively. The equilibrium magnetic field in the plasma is $\boldsymbol{B} = F\boldsymbol{\nabla}\phi - \boldsymbol{\nabla}\psi \times \boldsymbol{\nabla}\varphi$ where ψ is the poloidal flux. The plasma is described by the resistive MHD equations [17] (we normalise $\mu_0 = 1$) whereas the absence of currents in the vacuum region implies that $\boldsymbol{\nabla} \times \boldsymbol{B} = 0$. We denote with ρ and η the mass density and resistivity respectively, both assumed to be constant. The temperature is taken to be a decreasing function of the radius with $T_i = T_e = T$.

We adopt a magnetic separatrix so that $q \to \infty$ logarithmically at the edge (q is the safety factor) and assume that this divergence is well localised in an infinitesimally narrow region about the boundary. Far from the plasma-vacuum boundary region, q is piecewise continuous, constant for $0 < r < r_0$ (*core region*) with value $q_0 = m/n - \delta q > 1$. We take q_0 strictly above unity to avoid $m = n$ infernal type perturbations developing [15]. For $r > r_0$ (*external region*) we choose $q = q_0(r/r_0)^2$, extending into the vacuum region up to the ideally conducting wall located at $r = b$ (cf. Fig. 1-(a)). The presence of a separatrix forces any perturbation of helicity m/n to resonate within the plasma. In order to model this effect, we constrain the maximum width of the current channel r_0 so that for a given m and n we impose $(m+1)/n < q(a)$.

A sheared equilibrium toroidal MHD flow $\boldsymbol{u} = R^2\Omega(r)\boldsymbol{\nabla}\phi$ is allowed under the assumption of being sufficiently weak not to induce centrifugal corrections to equilibrium pressure and mass density profiles [18]. Both pressure and rotation profiles are parametrised by a Heaviside step-function H (cf. Fig. 1-(b))

$$p/p_0 = H(r_p - r), \quad \Omega/\Omega_0 = H(r_\Omega - r), \tag{1}$$

with $0 < r_p < r_0$ and $r_1 < r_\Omega < r_2$. Here p_0 and Ω_0 are the axis values of pressure and rotation respectively. Without loss of generality we take $\Omega_0 > 0$.

Let us fix the toroidal mode number n. In region $0 < r < r_0$ we allow for toroidicity driven coupling between a main mode ξ_m and its satellite harmonics $\xi_{m\pm1}$ with $\xi_{m\pm1} \sim \varepsilon\xi_m$ [14, 15]. Higher order harmonics are ignored. Hereafter ξ denotes the perturbation and any other quantity takes its equilibrium value. In this region plasma inertia is neglected and it is assumed that $(\delta q/q)^2 \sim \varepsilon\alpha$. By solving for ξ_{m+1} in the region $0 < r < r_0$ and imposing smooth matching across r_0 and regularity of the sidebands at the magnetic axis, an

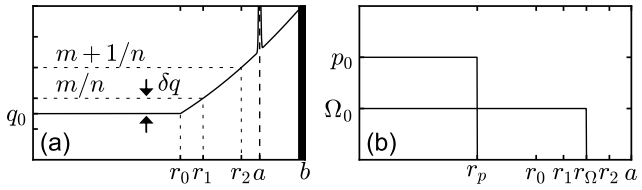

Figure 1. Safety factor (a), and pressure and toroidal rotation profiles (b) used in the following analysis. In panel (b), the units of the y-axis are arbitrary.

equation for ξ_m is found [15, 19, 20]

$$[r^3 Q\xi_m']' - r[(m^2-1)Q + \mathscr{D}_M]\xi_m + \frac{\alpha(1+m)}{2} \times \\ \times \frac{r^{1+m}}{r_0^{2+2m}}\left(\frac{2+m+c}{m-c}\right)\int_0^{r_0} r^{1+m}\alpha\xi_m dr = 0, \tag{2}$$

where $\alpha = -(2R_0 p' q^2)/B_0^2$, $Q = (\delta q/q)^2$, $\mathscr{D}_M = \alpha(1 - 1/q^2)r/R_0$, and $c = r_0\xi_{m+1}'(r_0)/\xi_{m+1}(r_0)$. Note that the coupling effectively involves only two harmonics, namely ξ_m and ξ_{m+1}. Toroidal rotation modifications to Q and $\mathscr{D}_M$, as the ones reported in Ref. [18], are neglected due to the weak flow assumption. If shaping effects are allowed, $\mathscr{D}_M$ is modified according to Ref. [19], and the last term in (2) weakened by an elongation dependent factor [19].

With the safety factor given above, the two resonances $q = m/n$ and $q = (m+1)/n$ occur at $r_1 = r_0(m/nq_0)^{1/2}$ and $r_2 = r_0[(m+1)/nq_0]^{1/2}$ respectively. No mode coupling occurs for $r_0 < r < a$ because of the large shear and the absence of strong pressure gradients (cf. (1)). Moreover, ξ_m must remain finite at r_1 to leading order and has to vanish at either the ideal wall or infinity. This forces $\xi_m = 0$ in the region $r > r_1$ [3]. We notice that even in the case $\xi_m \sim \xi_{m+1}$, coupling is of higher order. Thus we envisage that this reduced spectrum is sufficient to capture the key physical effects. Far from the resonances, ξ_ℓ ($\ell = m, m+1$) obeys equation [21]

$$\mathscr{L}_\ell\xi_\ell \equiv [r^3(\ell/q - n)^2\xi_\ell']' - r(\ell^2-1)(\ell/q-n)^2\xi_\ell = 0, \tag{3}$$

with general solution $\xi_\ell \propto (r^{\ell-1} + Nr^{-\ell-1})/(\ell/q - n)$ where N is a constant. This form of ξ_ℓ also solves (2) in region $0 < r < r_p$ and $r_p < r < r_0$ with the pressure profile given by (1) [8, 19].

The asymptotic behaviour of ξ_m near the resonance r_1 is $\xi_m \propto \frac{1}{x} \mp \Delta_{\pm,m}$ for $x \gtrless 0$ with $x = (r - r_1)/r_1$. The sideband ξ_{m+1} behaves similarly at r_2 with the obvious replacements $x \to (r - r_2)/r_2$ and $\Delta_{\pm,m} \to \Delta_{\pm,m+1}$.

The layer response is obtained by matching the solutions far from and close to the resonance, yielding $\ell\pi\Delta_{R,\ell} = -[\Delta_{-,\ell} + \Delta_{+,\ell}]$. This is used to express $\Delta_{-,\ell}$ as function of wall ($\Delta_{+,\ell}$) and layer ($\Delta_{R,\ell}$) responses. Wall physics is contained in the term $\Delta_{+,\ell}$, which is obtained

from the smooth matching of the solution of (3) with the vacuum one [22, 23]

$$\Delta_{+,\ell} = -\frac{1}{2} - \ell\frac{(r_{s,\ell}/b)^{2\ell} + 1 + 1/\gamma\tau_w}{(r_{s,\ell}/b)^{2\ell} - 1 - 1/\gamma\tau_w}, \qquad (4)$$

having employed the thin wall approximation [24], with τ_w denoting an effective wall diffusion time, $r_{s,m} = r_1$ and $r_{s,m+1} = r_2$. Note that $\Delta_{+,\ell}$ remains bounded unless $r_{s,\ell} \to b$, and for $b \to \infty$ its expression coincides with the one obtained letting τ_w finite and $\gamma \to 0$. This indicates that the stability limit computed with a resistive wall conforms to the one with the wall at infinity.

At r_1 we assume an ideal response

$$\Delta_{R,m} = -\frac{\omega_1}{\gamma - i\Omega_0} \quad \omega_1 = \frac{\omega_A s_1 n/m}{\sqrt{1 + 2m^2/n^2}}, \qquad (5)$$

where $\omega_A = B_0/R_0\sqrt{\rho}$ and s_1 the magnetic shear at position r_1. Notice that inertia at r_1 is enhanced by a factor $\sim \sqrt{2}(m/n)^2$. Note that in our model $s_1 = 2$, however if δq is sufficiently small, one could approximate $s_1 \approx n\delta q/m$ which is more appropriate for a smooth current profile.

We let $\Delta_{R,m} \gg \Delta_{+,m}$, i.e. sufficiently small γ, Ω_0 and $(r_2/b)^{2m}$. Since $T(r_2) < T(r_1)$, we allow for plasma resistivity at r_2. Equation (3) is augmented by a Glasser-Greene-Johnson (GGJ)-like term ν [16], that is $(\mathscr{L}_{m+1} - r_2 s^2 \nu)\xi_{m+1} = 0$ with $0 < \nu \ll 1$, and solved far from r_2 via a WKB expansion for small $1/(m+1)$ [25]. The resulting expression is joined asymptotically with the perturbative (in ν) solution of the equation above about r_2. The latter is finally matched with the layer solution [26]. In the limit of ν sufficiently small, this yields [16, 27]

$$\Delta_{R,m+1} = \frac{\Gamma(3/4)}{2\Gamma(5/4)}\frac{c_0^{1/2} S^{3/4}}{m+1}\left(\frac{\gamma}{\omega_A}\right)^{5/4}\left[1 + \frac{\pi\nu}{4M}\right], \qquad (6)$$

where $c_0 = \sqrt{1 + 2(m+1)^2/n^2}/(ns_2)$ with s_2 the magnetic shear at r_2, $S = a^2\omega_A/\eta$ is the Lundquist number, Γ is the Gamma function and $M = c_0(\gamma/\omega_A)^{3/2}S^{1/2}$. It is easily shown that with the choice of the safety factor given above, the tearing stability index of the mode $m+1$ is negative for an ideal wall at infinity. This guarantees that the system is stable against classical tearing modes [28].

We shall focus on the $n = 1$ mode. With the pressure profile given by (1), the dispersion relation is obtained by integrating (2) across r_p [18, 19], and joining smoothly at r_0 the core and external region solutions for ξ_m and ξ_{m+1}. This yields to first order in $1/\Delta_{R,m}$

$$\lambda_H + \frac{B}{\Delta_{R,m}} + \frac{A}{\Delta_{R,m+1} - \Delta'_T} = 0. \qquad (7)$$

λ_H measures the magnitude of the ideal growth rate and is well approximated by

$$\lambda_H \approx \frac{(1+m)\bar\beta^2}{2\varepsilon_p^2}\frac{(r_2/r_0)^{2+2m} - 2 - \delta q}{1 + \delta q(r_2/r_0)^{2+2m}}\left(\frac{r_p}{r_0}\right)^{2+2m} - \bar\beta(1 - 1/q_0^2) - \frac{2m(m-1)Q}{m - 1 + (m+1)(r_p/r_0)^{2m}},$$

with $\bar\beta = 2p_0 q_0^2/B_0^2$ and $\varepsilon_p = r_p/R_0$. The quantities A and B, both positive, are defined as

$$A = \frac{(m+1)\bar\beta^2}{\pi\varepsilon_p^2}\frac{(1+\delta q)^2(r_2 r_p/r_0^2)^{2+2m}}{[1 + \delta q(r_2/r_0)^{2+2m}]^2},$$

$$B \approx \frac{16m^3(r_p/r_1)^{2m}/(\pi q_0^2)}{[m - 1 + (m+1)(r_p/r_0)^{2m}]^2},$$

having neglected the weak dependence upon δq in $q_0^2 B$ (this holds if r_p/r_0 is not too close to unity). It is worth noticing that for $m = 2$ the factor q_0^2 appearing in the expression of B above, cancels out with the one contained in the definition of r_1. Finally, Δ'_T is written as

$$\pi(m+1)\Delta'_T = \frac{m + 1/2 - (m+3/2)\delta q(r_2/r_0)^{2+2m}}{1 + \delta q(r_2/r_0)^{2+2m}} - \Delta_{r,m+1},$$

which recovers the tearing mode stability index of mode $m+1$ at r_2 for δq sufficiently large. Notice that $\Delta'_T \le 0$ for $\delta q > 0$ in the ideal wall limit, i.e. $\tau_w \to \infty$. Thus, in order to extend the range of applicability of (7), we may regard Δ'_T as a free parameter, letting it vary from $-\infty$ to 0.

With no rotation, the ideal marginal boundary ($\Delta_{R,\ell} \to \infty$) is identified by $\lambda_H = 0$, and corresponds to the usual ideal-wall β limit. We see that in an ideal plasma there is no wall influence, neither ideal nor resistive, on the boundary due to the fact that the resonances of the modes involved occur within the plasma, leading to an effective screening of the wall effects. This holds true even if mode coupling is allowed in the region $r > r_0$ with ξ_{m+1} dominant over ξ_m. Moreover, the ideal marginal boundary is very weakly affected by non-vanishing rotation at r_2, if the flow is not too large, i.e. if the condition $\Delta_{R,\ell} \gg 1$ is fulfilled.

Allowing a tearing response at r_2 ($\Delta_{R,m+1} \sim \gamma^{5/4}$) with neither rotation nor GGJ effects, the stability limit is given by the relation $\lambda_H/A - 1/\Delta'_T = 0$, which occurs for $\lambda_H < 0$. We call this stability limit the *resistive β-boundary*. Stability is increasingly worsened as $\Delta'_T \to 0$, pushing the marginal boundary λ_H/A to $-\infty$, that is the mode is always unstable. The wall affects this boundary, and its effect becomes more pronounced as r_2 approaches b. This result can be generalised to the $\Delta'_T > 0$ case [29], showing that no threshold is present if $\nu = 0$. The marginal boundaries for the ideal and resistive case discussed above are shown in Fig. 2 in the $\beta_N - \delta q$ space

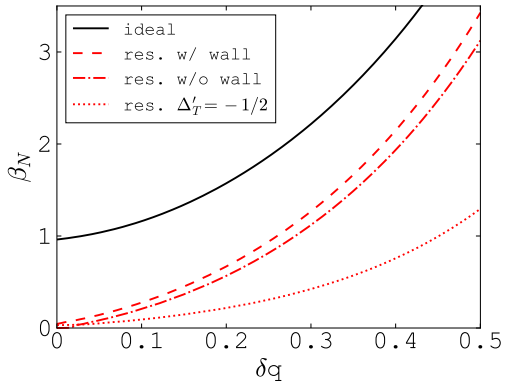

Figure 2. Ideal and resistive marginal boundaries for the $n = 1$ mode with a dominant $m = 2$ component with $r_0/a = 0.6$, $r_p/a = 0.35$ and $\varepsilon_p = r_p/R_0$ with $\varepsilon = a/R_0 = 1/3$. The unstable regions lie above each curve. The wall position of the stability curve of the resistive mode w/ wall is set at $b/a = 1.05$.

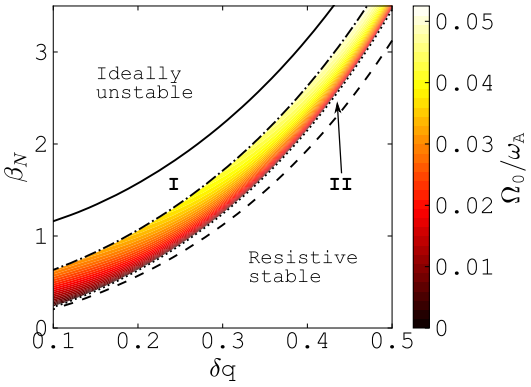

Figure 3. Contours of the critical rotation required to stabilise the resistive mode with the same parameters of Fig. 2 apart from $b \to \infty$ here. The ideal instability region lies above the solid curve, and the purely resistive mode is stable below the dashed one. Region `I` is ideally stable-resistive unstable. Region `II` is stable thanks to GGJ effects (here we take $\nu_* = 10\times\beta^{5/6}$). Equation (9) holds between regions `I` and `II`, below the $A/|\lambda_H|+\Delta'_T-\nu_* \approx 1$ level denoted by the dot-dashed line. The colours in this region indicate the required rotation for marginal resistive MHD stability. Smaller rotation frequency may be needed for smaller values of s_1.

with $\beta_N = \beta[\%]q(a)/(5\varepsilon)$ (computed in the cylindrical limit) and $\beta = \bar{\beta} r_p^2/(q_0 a)^2$. If $\nu \neq 0$, GGJ effects are expected to stabilise the resistive mode [16], effectively introducing an intermediate threshold between the ideal and resistive ones. We point out that a neoclassical drive must be added when the analysis is extended to the nonlinear phase.

Let us now assume that $\lambda_H < 0$, i.e. we analyse an ideally stable situation, and allow for a toroidal flow of the form given by (1). Since we are mostly interested in the marginal stability boundaries, we consider the case of wall at infinity ($b \to \infty$). We identify two roots: one which rotates with frequency close to Ω_0 (*fast-frequency root*), and the other with $|\gamma| \ll \Omega_0$ (*low-frequency root*). In the former case we write $\gamma = i\Omega_0 + \delta$ with $|\delta| \ll \Omega_0$, and substitute into (7). It is immediate to see that if $|\lambda_H|$ and $\Delta_{R,m+1}$ are sufficiently large, i.e. large Lundquist number, then $\mathrm{Re}(\delta) < 0$.

The low-frequency root is analysed recasting equation (7) by means of (5) as

$$\Delta_{R,m+1} = A\frac{|\lambda_H| + iB\Omega_0/\omega_1}{|\lambda_H|^2 + B^2(\Omega_0/\omega_1)^2} + \Delta'_T,$$

which is valid far from the ideal boundary, having approximated $\gamma - i\Omega \approx -i\Omega$ [9]. Using (6) in the limit of ν/M small and far from the resistive β-boundary, we get

$$\mathrm{Re}(\gamma) = \gamma_T\left[1 - \frac{\pi\nu}{5c_0 S^{1/2}}\left(\frac{\gamma_T}{\omega_A}\right)^{-3/2}\right] \qquad (8)$$

with the characteristic growth rate given by

$$\frac{\gamma_T}{\omega_A} = S^{-3/5}\left[\hat{C}_0\frac{m+1}{c_0^{1/2}}\left(\frac{A|\lambda_H|}{|\lambda_H|^2+\Omega_*^2} + \Delta'_T\right)\right]^{4/5},$$

where $\Omega_*^2 = B^2(\Omega_0/\omega_1)^2$ and $\hat{C}_0 = 2\Gamma(5/4)/\Gamma(3/4)$. This root grows on slow time scales, of the order of tens of milliseconds with ω_A of the order of megahertz. The $S^{-3/5}$ dependence of γ_T also makes the rotation frequency of the mode small compared to the one of the bulk plasma. Core plasma rotation provides a stabilising effect and its critical value obtained from (8) reads

$$\frac{\Omega_0}{\omega_1} = \frac{|\lambda_H|}{B}\sqrt{\frac{A/|\lambda_H|}{\nu_* - \Delta'_T} - 1} \qquad (9)$$

with $\nu_* \approx 0.41 \times \nu^{5/6}(s_2 S)^{1/3}/(m+1)^{4/3}$. Without rotation, the stability boundary of the resistive mode modified by GGJ effects at r_2 is identified by $A/|\lambda_H| - \nu_* + \Delta'_T = 0$. Close to this boundary, the rotation values needed to stabilise the mode can be of the order of few percent of the Alfvén frequency as shown in Fig. 3 (a linear dependence of ν upon β is chosen).

As ν_* is increased, the marginal curve approaches the ideal one ($\lambda_H = 0$) and the eigenfunction ξ_{m+1} changes its parity from tearing to kink-like. If $\Delta'_T > 0$, the marginal stability curve can be expressed in a form similar to (7) replacing $A \to \hat{A} > 0$. Thus, stabilisation occurs at larger values of ν_*, i.e. for smaller resistivity, leading us to infer a kink structure for the the marginal ξ_{m+1}. Moderate plasma shaping can be expected to improve stability due a modification of $\mathscr{D}_M$ and ν and mode coupling weakening [19, 30].

Similar conclusions can be drawn on internally non-

resonant cases with $q_0 > m/n$, as long as r_0/b remains small enough, for which lower β limits are envisaged due to a weakening of field line bending stabilising terms [19, 31]. For broader current profiles, the absence of the internal m/n resonance can lead to more pronounced wall effects on the stability.

In summary, we developed a simple model apt to describe macroscopic β-driven instabilities in a diverted tokamak. It predicts a slow growing, slow rotating mode driven unstable below the ideal-wall β limit by plasma resistivity. Stability is improved by the synergy of sheared toroidal rotation and GGJ effects, the former of the order of few percent of the Alfvén speed. We found that wall effects in an ideal plasma are screened by internal resonances, ruling out ideal external kinks as a possible drive of mode instability.

Fruitful discussions with Dr D. Dragoni are gratefully acknowledged. This work has received funding from Enabling Research grant on Operational Limiting Plasma Instabilities (CdP-FSD-AWP21-ENR-03). This work has been carried out within the framework of the EUROfusion Consortium, funded by the European Union via the Euratom Research and Training Programme (Grant Agreement No 101052200 — EUROfusion). Views and opinions expressed are however those of the author(s) only and do not necessarily reflect those of the European Union or the European Commission. Neither the European Union nor the European Commission can be held responsible for them. This work was supported in part by the Swiss National Science Foundation.

* Electronic address: daniele.brunetti@ukaea.uk

[1] H. Reimerdes *et al.*, Phys. Plasmas **13**, 056107 (2006).
[2] M. S. Chu and M. Okabayashi, Plasma Phys. Control. Fusion **52**, 123001 (2010).
[3] M. Takechi *et al.*, Phys. Rev. Lett. **98**, 055002 (2007).
[4] S. W. Haney and J. P. Freidberg, Phys. Fluids B **1**, 1637 (1989).
[5] J. M. Finn, Phys. Plasmas **2**, 198 (1995).
[6] R. Fitzpatrick, Phys. Plasmas **9**, 3459 (2002).
[7] R. Betti, Phys. Plasmas **5**, 3615 (1998).
[8] C. J. Ham *et al.*, Plasma Phys. Control. Fusion **53**, 025001 (2011).
[9] A. Bondeson *et al.*, Phys. Plasmas **6**, 637 (1999).
[10] Y. He *et al.*, Phys. Rev. Lett. **113**, 175001 (2014).
[11] A. H. Boozer, Phys. Plasmas **2**, 4521 (1995).
[12] M. Okabayashi *et al.*, Nucl. Fusion **49**, 125003 (2009).
[13] L. J. Zheng *et al.*, Phys. Plasmas **24**, 102503 (2017).
[14] L .E. Zakharov, Nucl. Fusion **18**, 335 (1978).
[15] R. J. Hastie and T. C. Hender, Nucl. Fusion **28**, 585 (1988).
[16] A. H. Glasser *et al.*, Phys. Fluids **18**, 875 (1975).
[17] R. D. Hazeltine and J. D. Meiss, *Plasma Confinement* (Addison-Wesley Publishing Company, Redwood City, 1992).
[18] C. Wahlberg *et al.*, Plasma Phys. Control. Fusion **55**, 105004 (2013).
[19] D. Brunetti *et al.*, Plasma Phys. Control. Fusion **62**, 115005 (2020).
[20] J. P. Graves *et al.*, Plasma Phys. Control. Fusion **64**, 014001 (2022).
[21] W. Newcomb, Ann. Phys. **10**, 232 (1960).
[22] V. D. Shafranov, Sov. Phys.-Tech. Phys. **15**, 175 (1970).
[23] J. A. Wesson, Nucl. Fusion **18**, 87 (1978).
[24] C. G. Gimblett *et al.*, Nucl. Fusion **26**, 617 (1986).
[25] C. C. Hegna and J. D. Callen, Phys. Plasmas **1**, 2308 (1994).
[26] D. Correa-Restrepo, Z. Naturf. a **37**, 848 (1982).
[27] D. Brunetti *et al.*, Nucl. Fusion **62**, 076016 (2022).
[28] H. P. Furth *et al.*, Phys. Fluids. **16**, 1054 (1973).
[29] D. Brunetti *et al.*, Plasma Phys. Control. Fusion **56**, 075025 (2014).
[30] C. Wahlberg, Phys. Plasmas **14**, 042506 (2007).
[31] E. J. Strait *et al.*, Nucl. Fusion **39**, 1977 (1999).